Optimal heat-reversible snap joints for frame-panel assembly in aluminum space frame automotive bodies

Mohammed Shalaby and Kazuhiro Saitou
Department of Mechanical Engineering, University of Michigan, Ann Arbor, MI, USA

Abstract

This paper presents a method for designing heat-reversible snap joints, locator-snap systems that detach non-destructively by heating a certain location of parts. It is expected to dramatically improve the recyclability of aluminum space frame (ASF) bodies by enabling clean separation of frames and body panels. Extending our previous work on the sequential design of the locators and heating area [1], the method simultaneously optimizes locators, heating area, and snaps for ensuring joint detachment with minimum heat and avoiding resonance due to vehicle vibration. A multi-objective genetic algorithm is utilized to search for Pareto optimal design alternatives.

Keywords

Design for disassembly, snap-fit joints, aluminum space frame

1 INTRODUCTION

Aluminum space frame (AFS) automotive bodies (Figure 1) are typically made of a network of extruded aluminum frames enclosed within metal or plastic body panels. They are lighter than the conventional steel bodies with comparable rigidity, realizing superior fuel efficiency [2, 3]. Since manufacturing AFS bodies requires more energy than steel bodies, closed-loop recycling of frame aluminum is highly desired [2-5]. However, frame aluminum can only be recycled to lower-grade cast aluminum, if contaminated by the foreign material residues occurred at the forced separation of the permanent joints between frames and panels during disassembly or shredding. To improve frame recycling to the same grade aluminum, therefore, it is essential to develop a joining method that allows easy, non-destructive and clean detaching of frames and panels at a desired time.

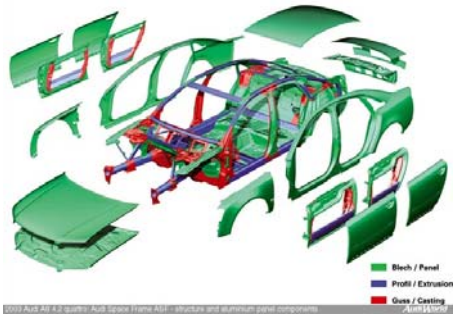

Figure 1: Audi Space Frame [4].

As a solution to this problem, we have previously introduced a concept of heat-reversible snap joints for automotive frame/panel assembly [1]. Figure 2 illustrates the concept. It is essentially a conventional locator-snap system found in literature [6], consisting of L-shaped locators and one or more snaps with truncated incline planes, molded or welded on the backside of a body panel. While assembled, the relative motion of the panel and frame is constrained by the locators wrapping around the frame and the snap locking into a catch, a square hole on a thin plate attached to the frame. Figure 3 shows the engagement steps, where the elasticity of the panel (and to some extent the catch) is exploited to enable the snapping action. This allows the locators to be stiff enough to meet the joints' structural requirements. Figure 4 illustrates the disengagement steps with heating, where in-plane thermal expansion constrained by locators, and to some extent the temperature gradient along the panel thickness, result in out-of-plane bulging of the panel that releases the snap.

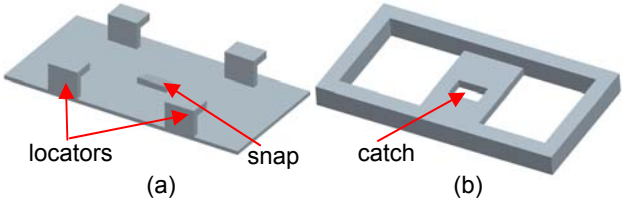

Figure 2: heat-reversible snap joint: (a) panel with four locators and a snap and (b) frame with a catch.

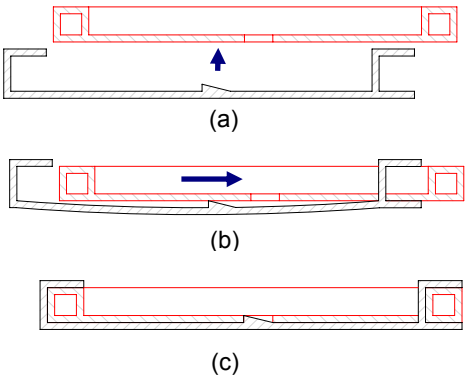

Figure 3: Engagement of heat-reversible snap: (a) push, (b) slide, and (c) lock.

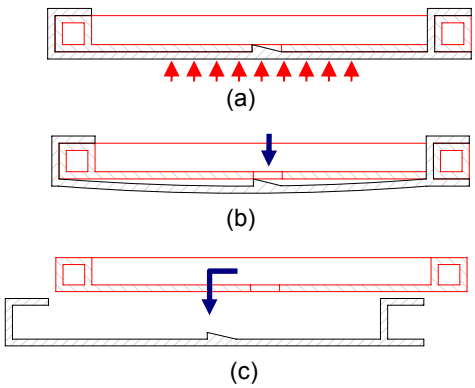

Figure 4: Disengagement of heat-reversible snap: (a) heat, (b) unlock, and (c) slide and remove.

Given the geometries of the panel and frame and the stiffness of the locators, our previous method [1] used sequential 2-step optimization to determine the number and locations of locators and the minimum heating area so that the panel does not resonate due to vehicle vibration while ensuring joint detachment. After the optimization, snaps are simply placed near the locations with the largest out-of-plane displacement during the heating. Since the 2-step optimization ignores the interaction among locators and heating area, it is unlikely to work for the complicated panel geometries of actual vehicles. To overcome this problem, this paper presents single step simultaneous optimization of the locators and heating area. A case study on an automotive panel/frame assembly with realistic panel geometry is presented.

2 RELATED WORK

2.1 Analysis and Design of Snap Fits

Analysis of specific types of snap fits, such as cantilever hooks, compressible hooks, bayonet fingers, etc can be found in [7-9]. More recently, integral attachments, including snap fits, were studied and classified into features based on functionality [10-12] and assembly motion [13]. Integral attachments were recommended as a joining method for design for disassembly in [14-16]. These works, however, did not address the reversible snap-fit designs that are actuated by thermal deformation.

2.2 Design for Disassembly with Reversible Joints

Chiodo *et al*. [17] developed the concept of active disassembly using smart materials (ADSM) that relies on self-disengaging fasteners and compression springs. Although the given examples were effective in the particular cases presented, the method lacks generality since it required the use of special and costly materials.

Li *et al.* reported topology optimization of reversible snaps [18-20]. Since the unlocking motions of these snap designs rely solely on the local transient thermal deformations of the snap, the opening actions are too small for practical applications. Heat-reversible snap designs presented in [1] and in this paper, overcome this problem by converting the in-plane thermal expansion of the panel constrained by locators to out-of-plane bulging that releases the snap.

3 METHOD

The method can be summarized as follows:

- **Given:** panel and frame geometry, feasible regions for locator placement, for snap placement, and for heating.
- **Find:** number, locations, and orientations of locators and snaps, area for heating.
- **Subject to:** realization of engagement actions in Figure 3 and disengagement actions in Figure 4, and structural requirements to the panel/frame assembly.
- **Minimizing:** number of locators and area for heating.

The method solves the above optimization problem in the following two steps:

1. Selection of locator and snap orientations for engagement.
2. Simultaneous optimization of locators and heating area for disengagement and structural requirements.

As in [1], snaps are simply placed near the locations with the largest out-of-plane displacement during the heating, in the orientation chosen in step 1. Noted that step 2 was solved in 2-step optimization in our previous work [1], with step 1 implicitly assumed as a given input.

3.1 Inputs

Inputs to the problem are panel and frame geometry, and feasible regions P_l, P_s *and* P_h in the panel for locator placement, for snap placement, and for heating, respectively. Figure 5 shows examples of these inputs.

The regions P_l, P_s *and* P_h are specified to incorporate spatial constraints, such as the existence of other components and the need of clearance for maintenance. The feasible region P_l for locator placement is the area in the panel that contacts the frame without such constraints. The feasible region P_s for snap placement is the non-contacting area of the panel where catches can be placed. The feasible region P_h for heating is the non-contacting area of the panel where the temperature just below the melting point of the panel can be applied. Since the out-of-plain bulging of the panel with complex curvature is highly unpredictable, it should be ideally chosen as the entire non-contacting area of the panel.

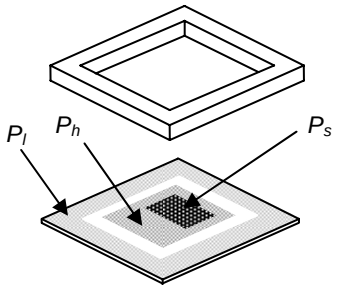

Figure 5: Examples of potential locator locations P_l, and region for snap placement P_s and for heating region P_h.

3.2 Selection of locator and snap orientations

To realize the engagement steps in Figure 3, the orientations of locators and snaps should be chosen, within their respective feasible regions, such that 1) the panel is under constrained before snapping and 2) the panel is fully constrained after snapping. While the locator orientations are constrained by the frame geometry, the snap orientations are arbitrarily chosen within P_s. Since both L-locators and snaps utilize plane-to-plane contacts to constrain the panel motion, translational degree of freedom, both in positive and negative directions, are of primal interests.

Figure 6 shows two examples where the above conditions for the joint engagement are satisfied. In Figure 6 (a), locators l_1, l_2 and l_3 constrain the panel motions in $+x$, $\pm y$, and $\pm z$ directions, but do not constrain $+x$ direction. After snapping, snap s_1 provides the constraint in this direction, thereby fully constraining the panel to the frame. Similarly, locators l_4 and l_5 in Figure 6 (b) constrain in $+x$, $-y$, and $\pm z$ directions, whereas snap s_2 constrain the rest of $-x$ and $+y$ directions to fully constrain the panel upon snapping.

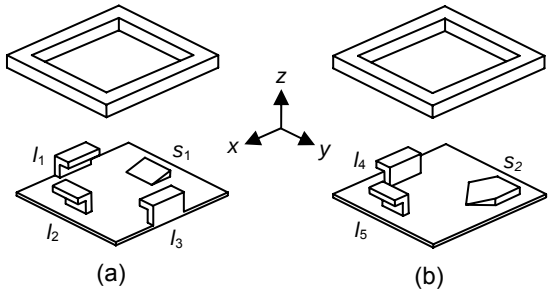

Figure 6: Example locator and snap orientations that fully constrain the panel to the frame.

The above conditions can be more precisely expressed using the Screw Theory. Adopting the wrench matrix representation similar to [21], for example, locators l_1, l_2 and l_3 and snap s_1 are represented as:

$$\mathbf{W}_{l_1} = \begin{pmatrix} 0 & -1 & 0 & 0 & 0 & 0 \\ 0 & 0 & 1 & 0 & 0 & 0 \\ 0 & 0 & -1 & 0 & 0 & 0 \end{pmatrix} \quad (1)$$

$$\mathbf{W}_{l_2} = \begin{pmatrix} -1 & 0 & 0 & 0 & 0 & 0 \\ 0 & 0 & 1 & 0 & 0 & 0 \\ 0 & 0 & -1 & 0 & 0 & 0 \end{pmatrix} \quad (2)$$

$$\mathbf{W}_{l_3} = \begin{pmatrix} 0 & 1 & 0 & 0 & 0 & 0 \\ 0 & 0 & 1 & 0 & 0 & 0 \\ 0 & 0 & -1 & 0 & 0 & 0 \end{pmatrix} \quad (3)$$

$$\mathbf{W}_{S_1} = \begin{pmatrix} 1 & 0 & 0 & 0 & 0 & 0 \end{pmatrix} \quad (4)$$

where each raw represents the directional (raw) vectors of the force and moment in the global coordinate frame, which can be supported by a mating surface in a locator or a snap. For example, the 1st row in Equation 1 has -1 at the 2nd column, indicating the upright surface of locator l_1 can support the force in $-y$ direction. Note moments (the 4th, 5th, and 6th columns) are ignored due to our primal concern on the translational degrees of freedom.

Based on the principle of virtual work, the forces and moments represented by wrench matrix $\mathbf{W} = (\boldsymbol{w}_1,\ldots,\boldsymbol{w}_n)^T$ constraints the motions represented by twist matrix $\mathbf{T} = (\boldsymbol{t}_1,\ldots,\boldsymbol{t}_m)^T$ if and only if there exists a negative component in every column of the virtual coefficient matrix [22]:

$$\Delta(\mathbf{W},\mathbf{T}) = \begin{pmatrix} \delta(\boldsymbol{w}_1,\boldsymbol{t}_1) & \cdots & \delta(\boldsymbol{w}_1,\boldsymbol{t}_m) \\ \vdots & \ddots & \vdots \\ \delta(\boldsymbol{w}_n,\boldsymbol{t}_1) & \cdots & \delta(\boldsymbol{w}_n,\boldsymbol{t}_m) \end{pmatrix} \quad (5)$$

where $\sigma(\boldsymbol{w},\boldsymbol{t})$ is the virtual coefficient of wrench $\boldsymbol{w} = (\boldsymbol{f}^T, \boldsymbol{m}^T)$ and twist $\boldsymbol{t} = (\boldsymbol{\omega}^T, \boldsymbol{v}^T)$:

$$\delta(\boldsymbol{w},\boldsymbol{t}) = \boldsymbol{v}\times\boldsymbol{f} + \boldsymbol{\omega}\times\boldsymbol{m} \quad (6)$$

Equivalently, this can be written as:

$$\text{fully-constrained}(\Delta(\mathbf{W},\mathbf{T})) = \begin{cases} \textit{true} & \text{if } \forall j, \exists i,\ \delta(\boldsymbol{w}_i,\boldsymbol{t}_j) < 0 \\ \textit{false} & \textit{otherwise} \end{cases} \quad (7)$$

Equation 6 gives a compact representation of the above two conditions for feasible locators and snap orientations:

$$\text{fully-constrained}(\Delta(\bigcup_{k\in L}\mathbf{W}_k, \mathbf{T}_{all})) = \textit{false} \quad (8)$$

$$\text{fully-constrained}(\Delta(\bigcup_{k\in L\cup S}\mathbf{W}_k, \mathbf{T}_{all})) = \textit{true} \quad (9)$$

where L and S are the sets of locators and snaps, respectively, and $\mathbf{W}_k$ is the wrench matrix of a locator (if $k \in L$) or a snap (if $k \in S$), and $\mathbf{T}_{all}$ is the twist matrix of all translational motions in $\pm x$, $\pm y$, and $\pm z$ directions:

$$\mathbf{T}_{all} = \begin{pmatrix} 0 & 0 & 0 & 1 & 0 & 0 \\ 0 & 0 & 0 & -1 & 0 & 0 \\ 0 & 0 & 0 & 0 & 1 & 0 \\ 0 & 0 & 0 & 0 & -1 & 0 \\ 0 & 0 & 0 & 0 & 0 & 1 \\ 0 & 0 & 0 & 0 & 0 & -1 \end{pmatrix} \quad (10)$$

Using Equations 1-3, for example, the locator and snap orientations in Figure 6 (a) give:

$$\Delta(\bigcup_{k\in\{l_1,l_2,l_3\}}\mathbf{W}_k, \mathbf{T}_{all}) = \begin{pmatrix} -1 & 1 & 0 & 0 & 0 & 0 \\ 0 & 0 & 1 & -1 & 0 & 0 \\ 0 & 0 & -1 & 1 & 0 & 0 \\ 0 & 0 & 0 & 0 & 1 & -1 \\ 0 & 0 & 0 & 0 & -1 & 1 \end{pmatrix} \quad (11)$$

Since the 2nd column has no negative entry, fully-constrained = *false*. It can be also shown that fully-constrained = *true* if $\mathbf{W}_{S1}$ is added. Similarly, the design in Figure 6 (b) also satisfies Equations 8 and 9.

For typical panel and frame geometries, more than one choice of locator and snap orientations satisfy Equations 8 and 9. Although the choice among alternative orientations should ideally be done by comparing the optimization results in step 2, the designer can pick one based on his/her engineering judgment. For example, between two designs in Figures 6 (a) and (b), the one in Figure 6 (a) is likely to yield stiffer joints in step 2, since the locators are placed along three edges of the panel.

Equations 8 and 9 do not prohibit multiple locators and/or snaps from constraining the same degree of freedom. While this may cause undesirable tolerance stackup, the dimensional tolerances of the panel and frame are assumed to be sufficiently small in the following case study. The issue of over constraint and tolerance stackup, however, will be addressed as a part of future work.

3.3 Simultaneous optimization of locators and heating area

To realize disengagement steps in Figure 4 and to satisfy structural requirements (*e.g.* vibration) to the joint, the number and locations of locators and the heating area are simultaneously optimized using finite element simulations of structural and thermal behaviors. There are two design variables:

- $\boldsymbol{x} = \{ x_1, x_2, \ldots, x_n \}$ is a vector of binary variable representing the existence (=1) or absence (=0) of locators at each finite element node in P_I
- $\boldsymbol{y} = \{ y_1, y_2, \ldots, y_n \}$ is a vector of the m vertices of the area to be heated.

Using $\boldsymbol{x}$ and $\boldsymbol{y}$, the optimization problem is written as:

minimize $\{ f_1(\boldsymbol{x}), f_2(\boldsymbol{y}) \}$

subject to

min_displacement($\boldsymbol{x}$,$\boldsymbol{y}$) > h

structural_requirements($\boldsymbol{x}$,$\boldsymbol{y}$)

$\boldsymbol{x}_i \boldsymbol{x}_{i+1} = 0$ if nodes i and i+1 are adjacent

$\boldsymbol{x} \in \{ 0, 1 \}^n$

$\boldsymbol{y} \in P_h^m$

where:

- $f_1(\boldsymbol{x}) = \sum x_i$ is the number of locators
- $f_2(\boldsymbol{y})$ is the number of finite element nodes in the area enclosed by vertices in $\boldsymbol{y}$
- min_displacement($\boldsymbol{x}$,$\boldsymbol{y}$) is the minimum out-of-plane thermal displacement in P_s
- h is the height of snaps plus small tolerance
- structural_requirements($\boldsymbol{x}$,$\boldsymbol{y}$) is the structural requirements on the frame/panel assembly while in use, such as minimum joint stiffness and resonance frequency

After optimization, snaps are simply placed near the locations with the largest out-of-plane thermal displacement in P_s, in the orientation obtained in step 1.

The evaluation of displacement(***x***,***y***) requires thermo-structural FE analysis, whereas the evaluation of structural_requirements(***x***,***y***) requires structural FE analysis only. Since the locators are very small compared to the panel, they are represented in the FE model as the equivalent springs. The properties of the equivalent springs are obtained by measuring the tip deflections of the locator in response to a unit load in in-plane and out-of-plane directions using finite element analysis, as shown in Figure 7.

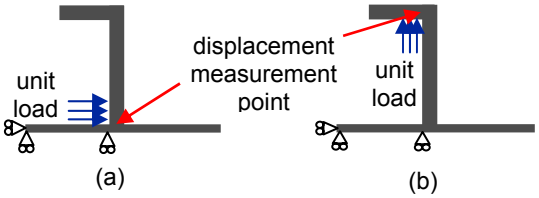

Figure 7: Measuring equivalent spring properties in (a) in-plane and (b) out-of-plane directions.

4 CASE STUDY

4.1 Inputs

Figure 8 shows a simplified automotive front fender panel and a frame. The fender panel is approximately 600 mm by 1000 mm, with a thickness of 3 mm, with J-shaped curvature along the top edge. It is made by injection-molding Nylon 66 with 30% glass (properties in Table 1). The frame (figure 8 (b)) is made of extruded aluminum square tubes with 25 mm external sides.

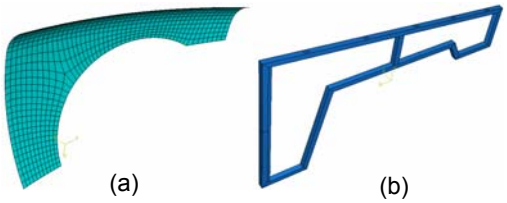

Figure 8: (a) front fender panel and (b) internal frame.

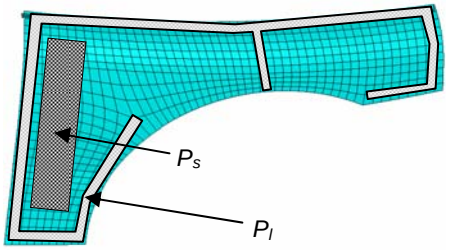

Figure 9: P_I and P_s for the fender panel. The entire panel is regarded as P_h.

Property Name (units)	Value
Density (g/cm3)	1.36
Elasticity modulus (MPa)	8500
Poisson Ratio	0.36
Melting point (^{o}C)	260
Thermal expansion coefficient (m/m.^{o}C)	3.00
Specific heat capacity (j/kg.^{o}C)	1800
Conductivity (W/m.^{o}K)	0.40

Table 1: Material properties of Nylon 66-30% glass filled.

Figure 8 shows the FE model of the fender panel with P_I, P_s. P_I contains 126 possible locator locations (n = 126). P_s chosen as a rectangle placed in the most flat area farthest from the frame. The entire panel is regarded as P_h.

4.2 Selection of locator and snap orientations

Based on the conditions in Equations 5 and 6, the orientations of locator and snaps are selected, by inspection, for each subregion of P_I and for P_s in Figure 9. The selected orientations are schematically illustrated (not in scale) in Figure 10. The locators along the curled top edge of the panel (grayed) lock into the slots on the frame, rather than wrap around the frame. It should be noted that Figure 10 only illustrate the orientations of locators and a snap at their representative locations in P_I and P_s. In particular, their placements do not represent the optimal number and locations to be obtained in step 2.

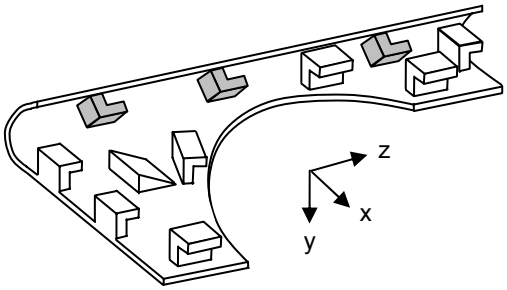

Figure 10: schematic of the orientations of locators and snaps (drawn not in scale) for the fender panel at the representative locations in P_I and P_s.

The panel can be attached to the frame (assumed stationary) by moving in –y, +x, and then +z direction. Upon unlocking of the snap with heating, the reverse motions can detach the panel from the frame.

4.3 Simultaneous optimization of locators and heating area

The dimensions of the locators are assumed constant everywhere in the panel, and chosen as in Figure 9 based on the standard injection molding guidelines [6]. This gives k_x = 4972.7 N/mm (in-plane), k_y = 5192.9 N/mm (out-of-plane).

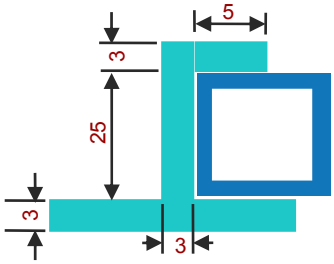

Figure 11: Locator dimensions for front fender panel. All dimensions are in mm.

For the thermo-structural simulation to calculate min_displacement(***x***, ***y***), the panel is heated at square area (m = 4) at 200^{o}C in the room of 20^{o}C. During heating, free convection to the air (convection heat transfer coefficient = 8 W/m^2.^{o}K) is considered as the only source of heat dissipation. The snap height h of 3 mm is used.

Since the aluminum frame carries majority of loads in AFS bodies, the structural requirements of the panels are typically for avoiding resonance to vehicle vibrations listed in Table 2 [23]. Accordingly, structural_requirements(***x***,***y***) is given as:

$$17 \le \omega_i(\boldsymbol{x}) \le 25 \quad \text{or} \quad 40 \le \omega_i(\boldsymbol{x}) \le 50 \quad \text{or} \quad 200 \le \omega_i(\boldsymbol{x}) \qquad (12)$$

where $\omega_i(\boldsymbol{x})$, i = 1, 2, …., 14, is the i-th natural frequency of the panel attached to the frame (considered as rigid) with the equivalent springs at the locations specified by $\boldsymbol{x}$.

The optimization problem is solved using multi-objective genetic algorithm (NSGA-II) [24]. Geometric and uniform crossovers are used, for $\boldsymbol{x}$, and heuristic and arithmetic crossovers are used for $\boldsymbol{y}$. Table 3 shows the parameters for NSGA-II. Since NSGA-II does not handle constraints explicitly, constraints are transformed to penalty functions that are treated as additional objective functions to be minimized:

$$f_3(\boldsymbol{x}, \boldsymbol{y}) = \{\max(0, h - \text{min\_displacement}(\boldsymbol{x}, \boldsymbol{y}))\}^2 \quad (13)$$

$$f_4(\boldsymbol{x}) = \sum_{i=1}^{14} p(\omega_i(\boldsymbol{x})) + \{\max(0,\ 200 - \omega_{14}(\boldsymbol{x}))\}^2 \quad (14)$$

where

$$p(\omega_i(\boldsymbol{x})) = \begin{cases} \left(\frac{17}{2}\right)^2 - \left(\frac{17}{2} - \omega_i(\boldsymbol{x})\right)^2 & \text{if } \omega_i(\boldsymbol{x}) < 17 \\ \left(\frac{15}{2}\right)^2 - \left(\frac{65}{2} - \omega_i(\boldsymbol{x})\right)^2 & \text{if } 25 < \omega_i(\boldsymbol{x}) < 40 \\ \left(\frac{150}{2}\right)^2 - \left(\frac{250}{2} - \omega_i(\boldsymbol{x})\right)^2 & \text{if } 50 < \omega_i(\boldsymbol{x}) < 200 \\ 0 & \text{otherwise} \end{cases} \quad (15)$$

These objective functions become zero when the constraints are satisfied.

Vibration source	Frequency range (Hz)
Suspension and wheels	5-10
Engine	11-17
Body	25-40
Driveline	50-150
Harshness	< 200

Table 2: vehicle vibration sources and frequency ranges.

Parameter	Value
Population size	130
Number of generations	140
Crossover probability	0.95
Mutation probability	0.05

Table 3: GA parameters used in this case study.

Figure 12 shows the Pareto optimal solutions for number of locators $f_1(\boldsymbol{x})$ and number of heated nodes $f_2(\boldsymbol{y})$, showing the trade-off between these objectives. All solutions in Figure 12 satisfy all the constraints, with the first natural frequency higher than 200 Hz. The second column in Table 4 shows the first 10 natural frequencies for Pareto solution 1 in Figure 12. For comparison, the third column of Table 5 shows the natural frequencies of the panel attached by bolted joints (i.e., rigid connection) at the same location. It can be seen that the frequency values with locators are comparable to the ones with bolted joint, indicating the high rigidity of the proposed heat-reversible snaps joints.

Figure 13 shows the locations of locators (circles), heating area (gray area), and snap (dark ellipse), and the deformed shape of Pareto solution 1 with the minimum number of locators. The number of locators is 24 and the heating area is 307x205 mm^2. The maximum and minimum out-of-plane displacements (Δ_y) within the heated zone are 5.608 mm and 3.018 mm, respectively. Therefore, snaps with 3 mm height can be located at the location of maximum deformation and guarantee opening. The in-plane displacements (Δ_x and Δ_z), which might potentially interfere the smooth unlocking of the snap, has the maximum value of 0.45 mm and are negligible compared to the out-of-plane displacement.

Similarly, Figure 14 shows the locations of locators, heating area, and snap, and the deformed shape of Pareto solution 5 with the minimum heating area. The number of locators is 28 and the heating area is 265 x 173mm^2. The maximum and minimum out-of-plane displacements (Δ_y) within the heated zone are 5.812 mm and 3.006 mm, respectively. Again, snaps that are 3 mm in height can be located at the center of the heated zone and guarantee opening. The in-plane displacements (Δ_x and Δ_z) has the maximum value of 0.48 mm and are negligible compared to the out-of-plane displacement.

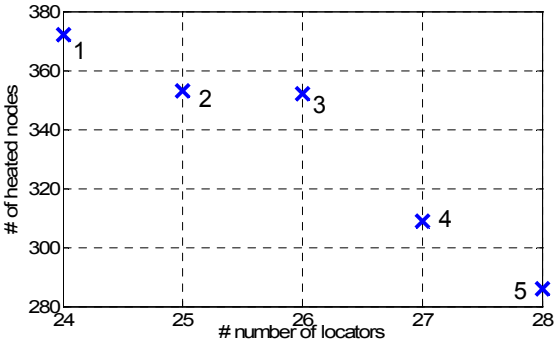

Figure 12: Pareto optimal solutions

Mode number	Frequency – locators (Hz)	Frequency – bolted (Hz)
1	200.70	252.17
2	208.88	272.18
3	212.16	278.18
4	233.01	283.31
5	245.30	303.37
6	257.78	340.22
7	271.54	344.77
8	274.36	352.74
9	286.16	404.36
10	331.00	417.34

Table 4: Natural frequencies of the fender panel with optimum locators (second column), and with bolted joints at the same location (third column)

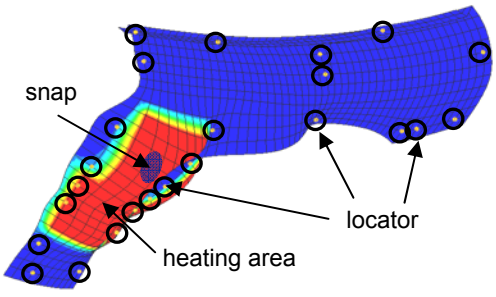

Figure 13: Pareto solution 1 with minimum number of locators (=24) and heated are = 307 X 205 mm^2

It is observed that the added complexity of the fender geometry, compared to [1], required more locators (24 compared to 19 in [1]) to achieve the same desired structural behavior.

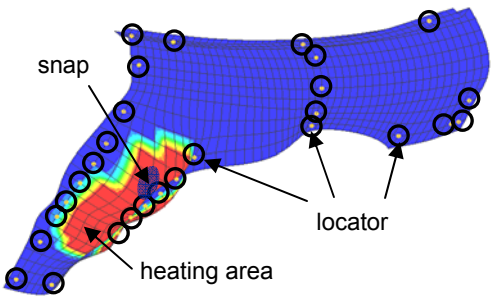

Figure 14: Pareto solution 5 with minimum heating area (=265 X 173 mm^2) and number of locators = 28.

5 CONCLUSION AND FUTURE WORK

This paper presented a design method for heat-reversible snaps, which allow easy, non-destructive, and clean detaching of internal frames and external panels in aluminum space frame automotive bodies. Future work includes simultaneous optimization of the orientations and locations of locators, addressing the issue of undesired tolerance stackup, and the extension to the frames with 3D geometry and other application areas.

ACKNOWLEDGMENTS

The authors gratefully acknowledge the funding provided by Toyota Motor Corporation, Japan, for this research.

REFERENCES

[1] Shalaby, M., Saitou, K., 2005, Design of Heat Reversible Snap Joints for Space Frame Bodies, Proceedings of the ASME Design Engineering Technical Conferences, September 24-28 Long Beach, CA, DETC2005-85155.

[2] Das, S., 2000, Life-Cycle Impacts of Aluminum Body-in-White Automotive Material, Journal of the Minerals, Metals & Materials Society, 52:41-44.

[3] “Design for aluminum recycling,” 1993, Automotive Engineering, 101:65-68.

[4] Audi world, http://www.audiworld.com

[5] Martchek, K., Fisher, E., Wasson, A., 1996, A Response to the Environmental Impact of Steel and Aluminum Body-in-Whites, Journal of the Minerals, Metals & Materials Society, 48:40-41.

[6] Bonenberger, Paul R., 2000, The First Snap-Fit Handbook, Creating Attachments for Plastic Parts, Hanser Gardner Publication, Inc., Cincinnati.

[7] Turnbull, V., 1984, Design Considerations for Cantilever Snap-Fit Latches in Thermoplastics, Proceedings of the Winter Annual Meeting of ASME, 84-WA/Mats-28, New Orleans, LA,:1-8.

[8] Wang, L., Gabriele, G., Luscher, A., 1995, Failure Analysis of a Bayonet-Finger Snap-Fit, Proceedings of the ANTEC ’95, May 7-11, Boston, MA: 799-3803.

[9] Larsen G., Larson, R., 1994, Parametric Finite-Element Analysis of U-Shaped Snap-Fits, Proceedings of the ANTEC ’94 May 1-5, San Francisco, CA: 3081-3084.

[10] Genc, S., Messler, R., Bonenberger, P., Gabriele, G., 1997, Enumeration of Possible Design Options for Integral Attachment Using a Hierarchical Classification Scheme, ASME Journal of Mechanical Design, 119:178-184.

[11] Genc, S. Messler Jr., R., Gabriele, G., 1998, A Systematic Approach to Integral Snap-Fit Attachment Design, Research in Engineering Design, 10:84-93.

[12] Genc, S. Messler Jr., R., Gabriele, G., 1998, A Hierarchical Classification Scheme to Define and Order the Design Space for Integral Snap-Fit Assembly, Research in Engineering Design, 10:94-106.

[13] Luscher, A., Suri G., Bodmann, D., 1998, Enumeration of Snap-Fit Assembly Motions, Proceedings of ANTEC ’98, April 26-30, Atlanta, GA: 2677-2681.

[14] Shetty, D., Rawolle, K., Campana, C., 2000, A New Methodology for Ease-of-Disassembly in Product Design, Recent Advances in Design for Manufacture (DFM), 109:39-50.

[15] Suri, G., Luscher, A., 1999, Structural Abstraction in Snap-fit Analysis, Proceedings of the ASME Design Engineering Technical Conferences, Las Vegas, Nevada, September 12-15, DETC99/DAC-8567.

[16] Nichols, D., Luscher, A., 1999, Generation of Design Data through Numerical Modeling of a Post and Dome Feature, Proceedings of the ASME Design Engineering Technical Conferences, Las Vegas, Nevada, September 12-15, DETC99/DAC-8596.

[17] Chiodo, J., Jones, N., Billett, E., Harrison, D., 2002, Shape Memory Alloy Actuators for Active Disassembly using Smart Materials of Consumer Electronic Products, Materials and Design, 23:471-478.

[18] Li, Y., Saitou, K., Kikuchi N., Skerlos, S., Papalambros, P., 2001, Design of Heat-Activated Reversible Integral Attachments for Product-Embedded Disassembly, Proceedings of the EcoDesign 2001, Tokyo, Japan, December 12–15:360–365.

[19] Li, Y., Saitou, K., Kikuchi, N., 2003, Design of Heat-Activated Reversible Integral Attachments for Product-Embedded Disassembly, International Journal of CAD/CAM, 3/1:26-40.

[20] Li, Y., Saitou, K., Kikuchi N., 2002, Design of Heat-Activated Compliant Mechanisms for Product-Embedded Disassembly, Proceedings of the Fifth World Congress on Computational Mechanics, Vienna, Australia, July 7-12.

[21] Lee, B. and Saitou, K., 2006, Three-Dimensional Assembly Synthesis for Robust Dimensional Integrity based on Screw Theory, Journal of Mechanical Design, 128/1:243-251.

[22] Marin, R., Ferreira, P., 2001, Kinematic analysis and synthesis of deterministic 3-2-1 locator schemes for machining fixtures, Journal of Manufacturing Science and Engineering, 123/4:708-719.

[23] Kasravi, K., Vehicle body design, TEC 452, Central Michigan University. www.kasravi.com/cmu/tec452/BodyEngineering/VibrationNoise.htm

[24] Deb, K., Pratap, A., Agarwal, S.; Meyarivan, T., 2002, A Fast and Elitist Multiobjective Genetic Algorithm: NSGA-II, IEEE Transactions on Evolutionary Computation, 6/2:182-197.

CONTACT

Kazuhiro Saitou

Department of Mechanical Engineering, University of Michigan, 2350 Hayward St., Ann Arbor, MI 48109-2125, USA, kazu@umich.edu.